

Soft Modes and Nonaffine Rearrangements in the Inherent Structures of Supercooled Liquids

Majid Mosayebi,^{1,*} Patrick Ilg,¹ Asaph Widmer-Cooper,² and Emanuela Del Gado³

¹*ETH Zürich, Department of Materials, Polymer Physics, CH-8093 Zürich, Switzerland*

²*School of Chemistry, University of Sydney, New South Wales 2006, Australia*

³*ETH Zürich, Department of Civil, Environmental and Geomatic Engineering, CH-8093 Zürich, Switzerland*

(Received 1 March 2013; revised manuscript received 13 December 2013; published 13 March 2014)

We find that the hierarchical organization of the potential energy landscape in a model supercooled liquid can be related to a change in the spatial distribution of soft normal modes. For groups of nearby minima, between which fast relaxation processes typically occur, the localization of the soft modes is very similar. The spatial distribution of soft regions changes, instead, for minima between which transitions relevant to structural relaxation occur. This may be the reason why the soft modes are able to predict spatial heterogeneities in the dynamics. Nevertheless, the very softest modes are only weakly correlated with dynamical heterogeneities and instead show higher statistical overlap with regions in the local minima that would undergo nonaffine rearrangements if subjected to a shear deformation. This feature of the supercooled liquid is reminiscent of the behavior of nonaffine deformations in amorphous solids, where the very softest modes identify the loci of plastic instabilities.

DOI: 10.1103/PhysRevLett.112.105503

PACS numbers: 61.43.Fs, 05.20.Jj, 64.70.Q-

Predicting the dynamical and mechanical behavior of simple liquids and crystalline solids from their structural properties can be successfully addressed by kinetic theories and elasticity, but this is not the case for glasses. Structurally, glasses and amorphous solids can be considered quite similar to supercooled liquids, but identifying a common link in their theoretical description is a major challenge. In both cases, the underlying potential energy landscape (PEL) is characterized by low-frequency normal modes that are quasilocalized in space [1–5]. These soft modes represent the flattest directions near minima in the PEL and appear to play a primary role in both the dynamics of supercooled liquids and the mechanics of amorphous solids [6–15]. In supercooled liquids, the soft modes are microscopically correlated with dynamical heterogeneities (DH) and irreversible rearrangements. Studies of model amorphous solids subjected to quasistatic shear have also shown that the lowest frequency normal modes can predict the spatial location of plastic events and extended shear bands in amorphous solids just prior to the event occurring [12,16,17]. These findings raise the question of whether the properties of supercooled liquids and amorphous solids are controlled by similar features of the PEL. For example, could slowing down of the liquid dynamics and the presence of plastic instabilities in amorphous solids be controlled by the same soft modes?

Here we investigate the spatial distribution of soft modes in a model supercooled liquid and find evidence that the time-scale separation typical of glassy dynamics can be ascribed to a qualitative change in the spatial distribution of the structurally soft regions. Nearby minima, which should lie within the same metabasin (MB; i.e., clusters of minima grouped together by rapid reversible dynamic transitions

between them), have very similar soft-mode localization. Instead, the mode localization appears to change significantly between MBs. We sample nearby minima by applying a shear deformation to a local minimum, or inherent structure (IS), of the PEL and find that regions undergoing nonaffine displacements between minima are also correlated with the spatially heterogeneous dynamics associated with the initial configuration. These nonaffinely rearranging domains overlap strongly with the softest normal modes in a manner similar to nonaffine deformations in amorphous solids, where the softest modes have been shown to identify the loci of plastic instabilities. These findings suggest that the soft modes and nonaffinely rearranging regions of the local minima represent the spatially resolved features of the PEL that link supercooled liquids and amorphous solids.

We study a model fragile glass former, a two-dimensional equimolar binary mixture of soft disks interacting via the purely repulsive potential $\phi(r) = \epsilon(\sigma_{ab}/r)^{12}$, where $\sigma_{12} = 1.2\sigma_{11}$ and $\sigma_{22} = 1.4\sigma_{11}$ [6,7,18]. We use 50 statistically independent samples of size ranging between $N = 2000$ and $N = 8000$ particles, equilibrated at temperatures spanning the supercooled regime of dynamics (between $T = 2.0$ and $T = 0.36$). All quantities are reported in reduced units, with the length and energy scale σ_{11} and ϵ , respectively. For $T < 0.36$, we could not reach full equilibration.

We start by comparing the spatial localization of soft regions in nearby configurations. To identify the structurally soft regions of each initial equilibrated configuration $X = \{\mathbf{r}_i\}$, we use the isoconfigurational Debye-Waller factor (DWF). This is defined for each particle i as the

variance of its position during a time interval $t_{\text{DW}} = 10\tau$, which corresponds to the short-time β -relaxation regime at $T = 0.4$, averaged over multiple runs originating from X . In supercooled liquids, this quantity has been shown to be spatially correlated with the soft-mode localization in the IS $X^q = \{\mathbf{r}_i^q\}$ belonging to X [6,7]. Starting from X , we sample nearby minima by computing the IS $X^{\text{dq}} = \{\mathbf{r}_i^{\text{dq}}\}$ of the deformed configuration $\mathbf{r}_i^{\text{d}}(\gamma) = \mathbf{r}_i + \gamma y_i \mathbf{e}_x$, using conjugate gradient minimization. Here γ is the magnitude of a planar shear deformation, applied following the procedure in Refs. [19,20]. The soft modes of X^{dq} are obtained by analyzing the local curvature of the PEL at $\{\mathbf{r}_i^{\text{dq}}\}$ by diagonalizing the Hessian matrix to obtain the $2N$ eigenfrequencies $\{\omega_j\}$ and the normalized eigenmodes $\{\mathbf{e}_{\omega_j}\}$. To characterize the soft-mode localization, we calculate the participation fraction of each particle i in each eigenmode \mathbf{e}_{ω_j} as $f_i^j = |\tilde{e}_{\omega_j}^i|^2$ (where $\tilde{e}_{\omega_j}^i$ is the displacement of particle i along the eigenmode \mathbf{e}_{ω_j}) and sum this over the N_m lowest frequency modes to obtain $p_i = \sum_{j=3}^{N_m} f_i^j$. Note that we have excluded the two zero-frequency modes (with index $j = 1, 2$) associated with the translational motion of the center of mass.

Figure 1(a) shows the magnitude of the statistical overlap $O_{\text{DW},p^{\text{dq}}}$ between the DWF of the initial configuration X and the soft-mode localization in the IS of the deformed configuration X^{dq} as a function of γ . Throughout the Letter, for properties A and B belonging to the same configuration, we define their overlap as $O_{A,B} = 2(N_A + N_B)^{-1} \sum_{j=1}^N \Theta(A_j) \Theta(B_j)$, where A_j is the value of quantity A for particle j , $N_A = \sum_j \Theta(A_j)$ and $N_B = \sum_j \Theta(B_j)$. $\Theta(A_j) = 1$ if the value of A_j is within the top 25% and belongs to a cluster of more than two particles that satisfy this criterion, otherwise $\Theta(A_j) = 0$ [6]. Error bars are given by the standard deviation over our 50 independent samples. In Fig. 1(a), for small γ , the overlap $O_{\text{DW},p^{\text{dq}}}$ is essentially independent of γ and increases as the temperature is lowered. However, the overlap drops as γ is increased beyond $\gamma_c \approx 0.071 \pm 0.024$. This value appears to be independent of temperature and system size, indicating that, over the entire landscape influenced regime of temperature, the spatial distribution of structurally soft regions does not change significantly until γ_c . This transition is accompanied by other changes in the properties of X^{dq} [see Fig. 1(b)]. For small γ , the IS energy $e_{\text{IS}}(\gamma)$ is approximately constant but starts to increase around the same value of γ where the overlap $O_{\text{DW},p^{\text{dq}}}$ decreases. This shows that deformation magnitudes of the order of γ_c push the system into local minima that are energetically less favorable than those sampled by thermal fluctuations. We also find that the increase in the IS energy is accompanied by a rapid increase in the average shear stress $\sigma_{xy}^{\text{dq}}(\gamma)$ of X^{dq} (see Fig. 1, inset), which reaches a maximum around γ_c , before dropping back to a value close to zero [21]. These results support the conclusion that γ_c is a characteristic property of the PEL.

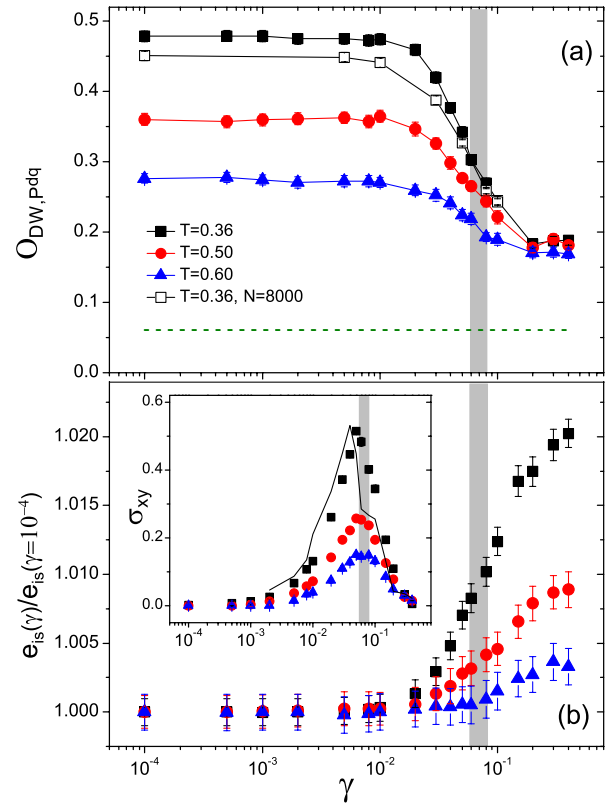


FIG. 1 (color online). (a) $O_{\text{DW},p^{\text{dq}}}$ as a function of the shear magnitude γ . $N = 2000$ particles (filled symbols) and $N = 8000$ particles (open symbols). The dashed line is $O_{\text{DW,RND}}$, the overlap with a randomly distributed variable, for $N = 2000$. (b) The normalized average IS energy e_{IS} as a function of γ . (Inset) Average shear stress σ_{xy}^{dq} for X^{dq} as a function of γ . The solid line is $de_{\text{IS}}/d\gamma$ at $T = 0.36$.

The change in the spatial distribution of soft regions that is captured by γ_c provides a new perspective on the hierarchical structure of the amorphous PEL. On the side of dynamics, the observation of frequent recrossings between nearby ISs has led to the concept of MBs, defined as the collection of minima connected by transitions with greater than a 50% probability of return [3,22]. Transitions between MBs have since been identified with higher energy barriers and local irreversible cage-breaking events [3,23–25]. The spatial pattern of DH, which is correlated with the soft-mode localization, has also been shown to change upon transitions between MBs [6,23,26]. Hence, the change in the spatial distribution of soft modes that we detect for $\gamma > \gamma_c$ could be related to MB transitions. Indeed, the value of γ_c that we calculate is similar in magnitude to the typical distance found for the separation between MBs [22,27,28]. On the side of mechanics, recent work on sheared amorphous solids [29] suggests that γ_c may also be related to the onset of irreversible mechanical relaxation processes. A transition from reversible particle motion to diffusive behavior is in fact detected at a critical shear amplitude of 0.07, very close to γ_c . Overall, our results

suggest that relaxation processes that have a low probability of being reversed in supercooled liquids and in sheared glasses may well be associated with a change in the spatial distribution of structurally soft regions.

To better understand the implications for the supercooled dynamics of the correlations we detect for $\gamma < \gamma_c$, we quantify the spatial distribution of DH at each T using the dynamic propensity (DP). The DP is defined for each particle i as the isoconfigurational average of its squared displacement $DP_i = \langle (\mathbf{r}_i(t_\alpha) - \mathbf{r}_i(0))^2 \rangle_{\text{iso}}$ over a time interval t_α that probes the α -relaxation regime [30]. In Fig. 2, we plot the overlap between the spatial distribution of the DP in X and the spatial distribution of soft-mode localization in X^q and in the nearby IS X^{dq} for $\gamma = 10^{-4}$, respectively, indicated as O_{DP,p^q} and $O_{\text{DP},p^{\text{dq}}}$. The data for O_{DP,p^q} expand on previous results [6,7] by showing that the overlap between the propensity and the soft-mode localization increases strongly in the landscape-influenced regime of the dynamics [31]. The statistical overlap $O_{\text{DP},p^{\text{dq}}}$ is also very similar to O_{DP,p^q} , indicating that the soft-mode localization in nearby ISs has a similar degree of spatial correlation with DH. The emerging picture is that the soft modes of the initial IS are able to predict the spatial pattern of DH occurring over time scales where the system visits many different minima because of the very similar soft-mode pattern of minima belonging to the same MB.

To extend these observations to lower temperature, we also consider the overlap O_{DW,p^q} since the DWF is less computationally demanding and spatially correlated with the DP [30]. O_{DW,p^q} initially behaves similar to O_{DP,p^q} but, at the lowest temperatures where we can equilibrate the system, stops increasing and approaches a plateau. This suggests a crossover to a regime where the structural

contribution to DH stops increasing, consistent with recent findings on dynamical correlation lengths [32].

When sampling nearby ISs using a shear deformation of amplitude γ , one can also identify the regions that undergo nonaffine displacements (NADs). The NAD field $\{\mathbf{d}_i\}$ is defined as the difference between the ISs belonging to the initial configuration X and the final configuration X^{d} when the affine deformation is subtracted, i.e., $\mathbf{d}_i(\gamma) = \mathbf{r}_i^{\text{dq}}(\gamma) - \mathbf{r}_i^q - \gamma y_i^q \mathbf{e}_x$. In amorphous solids, the NAD field is spatially correlated with the lowest energy soft modes, the evolution of which can predict the emergence of a local plastic instability in the material [16]. In supercooled liquids, the NAD field contains long-range correlations that increase in size upon approaching the glass transition [20,33]; however, a direct correlation with the soft modes and with the dynamics has not yet been established. In Fig. 2, we show the statistical overlap between the spatial distribution of DH and of the magnitude of the NAD field $O_{\text{DW},|\mathbf{d}|}$ measured for $\gamma = 10^{-4}$. This overlap is significantly higher than the one with a randomly distributed variable $O_{\text{DW},\text{RND}}$ and clearly increases upon entering the landscape-influenced regime, albeit not as strongly as the overlap of the DH with the soft modes. This result raises the question of whether there might be a correlation between the soft regions where DHs are more likely to appear in the supercooled liquid and the regions prone to plastic events once the system has solidified.

Figure 3 shows, for a typical supercooled liquid configuration, the spatial distribution of the DWF (top left), the magnitude of the NAD field $|\mathbf{d}|$ (top right), and the spatial distribution of the soft mode localization in the IS X^q (lower panels) summed over approximately 1.5% (left) and 0.1% (right) of the lowest frequency normal modes. We note that at low temperatures the NAD field shows characteristic quadrupolar patterns, typical of NADs in amorphous solids, in agreement with recent findings [34]. The maps in Fig. 3 reveal the significant correlations between the DWF, the NAD field, and the soft-mode localization that we have discussed so far. Interestingly, they also suggest that DH and NAD are sensitive to different subsets of the soft modes.

We have quantified these differences by computing the overlaps $O_{|\mathbf{d}|,p^{\text{dq}}}$ and $O_{\text{DW},p^{\text{dq}}}$ as a function of the number of low-frequency modes N_m included in the participation sum p^{dq} used to determine the soft-mode localization. The main part of Fig. 4 shows these overlaps in the deeply supercooled region ($T = 0.40$) for a small $\gamma = 10^{-4}$. We find that the DWF overlap $O_{\text{DW},p^{\text{dq}}}$ increases with N_m until 160 modes are included, whereas the NAD overlap $O_{|\mathbf{d}|,p^{\text{dq}}}$ decreases from an initial plateau. That is, about 1% of the lowest frequency normal modes makes a significant contribution to DH, whereas only the very lowest frequency nontrivial modes have similar spatial structure to the magnitude of the NAD field. These results suggest that the regions where structural relaxation is most likely to

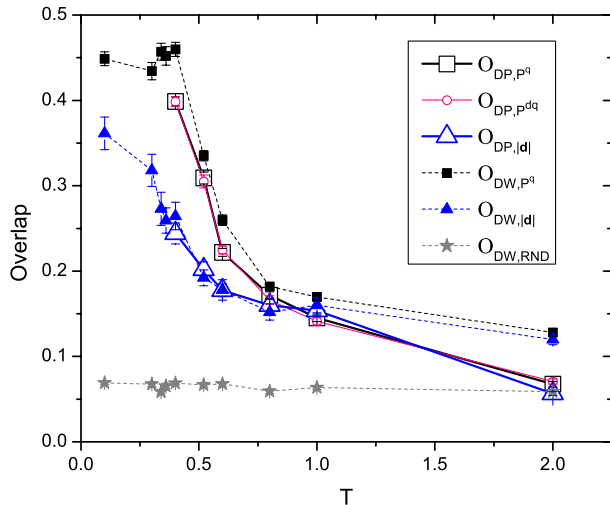


FIG. 2 (color online). Temperature dependence of the spatial correlation between DHs and some properties of the underlying PEL, as defined in the text. For the nonaffine displacements (NADs), we use $\gamma = 10^{-4}$, and for the soft mode localization, we use 1% ($N_m = 160$) of the lowest frequency modes.

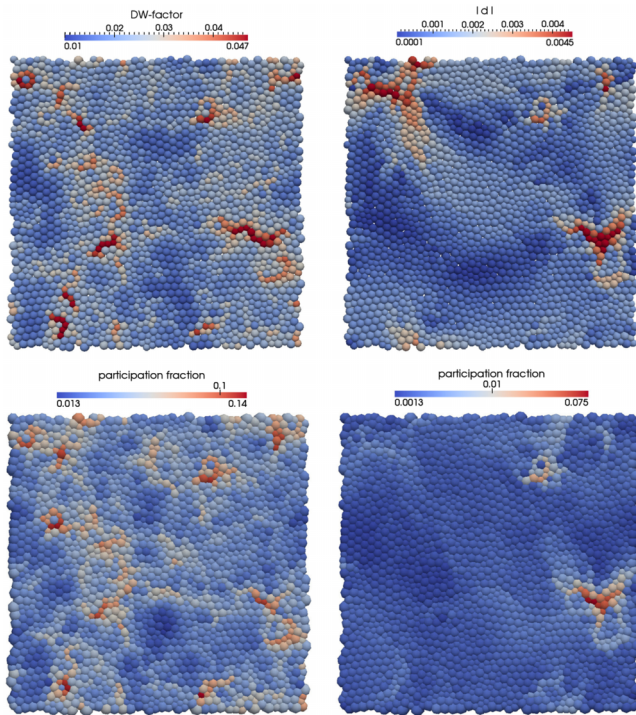


FIG. 3 (color online). (Top) Maps of the local Debye-Waller factor (left) and NAD magnitude (right) for the same initial configuration of $N = 2000$ particles at $T = 0.36$. For NADs, we used $\gamma = 10^{-4}$. (Bottom) Maps of the soft mode localization $\{p_i\}$ for X^q , the initial IS, with $N_m = 60$ (left) and $N_m = 7$ (right) of the lowest frequency modes included.

occur in the supercooled liquid can be quite distinct from the regions in which local plastic instabilities tend to occur in the amorphous solid. Interestingly, we also find that around γ_c the overlap between NAD and the soft modes of

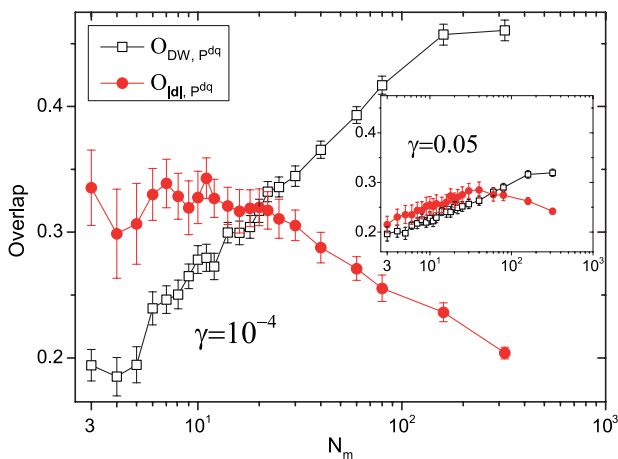


FIG. 4 (color online). Spatial overlaps between the soft modes of the final IS and, respectively, the DWFs (open) and the NADs (filled), as a function of the number of modes included in the sum over participation fractions, for a system of $N = 8000$ particles at $T = 0.40$. Main frame: $\gamma = 10^{-4}$; inset: $\gamma = 0.05$.

the IS after deformation is no longer sensitive to only the lowest frequency modes but instead exhibits a behavior more similar to the DWF overlap, as shown in the inset of Fig. 4.

In summary, we have provided new insight into the role of the spatial distribution of soft modes for the dynamics of supercooled liquids and explored the link that the modes provide with the amorphous solid eventually formed at the glass transition. Our work suggests that the separation between fast-reversible and slow-irreversible relaxation processes, usually associated with the hierarchical organization of the PEL, can be related to a qualitative change in the spatial distribution of soft modes among MBs. By investigating nonaffinely rearranging regions of the IS in the supercooled liquid, we find evidence that the soft modes relevant for DH can be quite distinct from the ones associated with the mechanical behavior of the solid. Elucidating the nature and origin of this difference can be important to reach deeper understanding and control of the liquid or solid properties of materials close to the glass transition and is an interesting subject for future work.

The computational resources of the PolyHub virtual organization are greatly acknowledged. A. W. was supported by the Australian Research Council and the Swiss National Science Foundation (Grant No. IZK0Z2_141601). P. I. acknowledges support from SNSF (Grant No. 200021_134626). E. D. G. is supported by the SNSF (Grant No. PP002_126483/1).

*Present address: Physical and Theoretical Chemistry Laboratory, University of Oxford, Oxford OX1 3QZ, United Kingdom.

- [1] M. Goldstein, *J. Chem. Phys.* **51**, 3728 (1969).
- [2] F. H. Stillinger, *Science* **267**, 1935 (1995).
- [3] A. Heuer, *J. Phys. Condens. Matter* **20**, 373101 (2008).
- [4] H. R. Schober and G. Ruocco, *Philos. Mag.* **84**, 1361 (2004).
- [5] S. Abraham and P. Harrowell, *J. Chem. Phys.* **137**, 014506 (2012).
- [6] A. Widmer-Cooper, H. Perry, P. Harrowell, and D. R. Reichman, *Nat. Phys.* **4**, 711 (2008).
- [7] A. Widmer-Cooper, H. Perry, P. Harrowell, and D. R. Reichman, *J. Chem. Phys.* **131**, 194508 (2009).
- [8] G. M. Hocky and D. R. Reichman, *J. Chem. Phys.* **138**, 12A537 (2013).
- [9] K. Chen, M. L. Manning, P. J. Yunker, W. G. Ellenbroek, Z. Zhang, A. J. Liu, and A. G. Yodh, *Phys. Rev. Lett.* **107**, 108301 (2011).
- [10] A. Ghosh, V. Chikkadi, P. Schall, and D. Bonn, *Phys. Rev. Lett.* **107**, 188303 (2011).
- [11] C. Brito and M. Wyart, *J. Stat. Mech. Theor. Exp.* **2007**, L08003 (2007).
- [12] C. E. Maloney and A. Lemaître, *Phys. Rev. E* **74**, 016118 (2006).
- [13] M. Tsamados, A. Tanguy, C. Goldenberg, and J.-L. Barrat, *Phys. Rev. E* **80**, 026112 (2009).

- [14] D. Rodney, A. Tanguy, and D. Vandembroucq, *Model. Simul. Mater. Sci. Eng.* **19**, 083001 (2011); A. Zaccone and E. Scossa-Romano, *Phys. Rev. B* **83**, 184205 (2011).
- [15] L. Yan, G. Düring, and M. Wyart, *Proc. Natl. Acad. Sci. U.S.A.* **110**, 6307 (2013).
- [16] A. Lemaître and C. Caroli, *Phys. Rev. E* **76**, 036104 (2007).
- [17] S. Karmakar, A. Lemaître, E. Lerner, and I. Procaccia, *Phys. Rev. Lett.* **104**, 215502 (2010).
- [18] D. N. Perrera and P. Harrowell, *J. Chem. Phys.* **111**, 5441 (1999).
- [19] E. Del Gado, P. Ilg, M. Kröger, and H. C. Öttinger, *Phys. Rev. Lett.* **101**, 095501 (2008).
- [20] M. Mosayebi, E. Del Gado, P. Ilg, and H. C. Öttinger, *Phys. Rev. Lett.* **104**, 205704 (2010).
- [21] See Supplemental Material at <http://link.aps.org/supplemental/10.1103/PhysRevLett.112.105503> for more details on the stress calculations.
- [22] B. Doliwa and A. Heuer, *Phys. Rev. E* **67**, 031506 (2003).
- [23] T. F. Middleton and D. J. Wales, *Phys. Rev. B* **64**, 024205 (2001).
- [24] V. K. de Souza and D. J. Wales, *J. Chem. Phys.* **129**, 164507 (2008).
- [25] V. K. de Souza and D. J. Wales, *J. Chem. Phys.* **130**, 194508 (2009).
- [26] G. A. Appignanesi, J. A. Rodriguez Fris, R. A. Montani, and W. Kob, *Phys. Rev. Lett.* **96**, 057801 (2006).
- [27] S. S. Ashwin, Y. Brumer, D. R. Reichman, and S. Sastry, *J. Phys. Chem. B* **108**, 19703 (2004).
- [28] The typical distance found for the separation between MBs in configuration space in Ref. [22] was about one particle diameter for a system of 65 particles, corresponding to $\gamma = 1/65 \approx 0.015$.
- [29] D. Fiocco, G. Foffi, and S. Sastry, *Phys. Rev. E* **88**, 020301 (2013); *Phys. Rev. Lett.* **112**, 025702 (2014).
- [30] A. Widmer-Cooper and P. Harrowell, *Phys. Rev. Lett.* **96**, 185701 (2006).
- [31] At high temperature, the DWF no longer measures particle localization, but our results are robust when t_{DW} is changed from 10τ to τ .
- [32] W. Kob, S. Roldán-Vargas, and L. Berthier, *Nat. Phys.* **8**, 164 (2012).
- [33] M. Mosayebi, E. Del Gado, P. Ilg, and H. C. Öttinger, *J. Chem. Phys.* **137**, 024504 (2012).
- [34] J. Chatteraj and A. Lemaître, *Phys. Rev. Lett.* **111**, 066001 (2013).